Available online at www.sciencedirect.com
ScienceDirect
J. Chem. Thermodynamics 40 (2008) 724–734
JCT
www.elsevier.com/locate/jct

Thermodynamic assessment of the phase equilibria in the Al–Ca–Sr system using the modified quasichemical model

M. Aljarrah, M. Medraj *

Department of Mechanical Engineering, Concordia University, 1455 de Maisonneuve Boulevard West, Montreal, Canada H3G 1M8

Received 29 June 2007; received in revised form 1 October 2007; accepted 4 October 2007
Available online 17 October 2007

Abstract

A thermodynamic description of the Al–Ca–Sr system is carried out using the modified quasichemical model. The three binary systems Al–Ca, Al–Sr, and Ca–Sr have been re-optimised based on the experimental phase equilibria and thermodynamic properties available in the literature. Good agreement was obtained for the calculated binary phase diagrams and their thermodynamic properties. The established database of this system predicted one saddle point, one peritectic, seven quasi-peritectics, and two ternary eutectics.

Keywords: Ternary phase diagram; Thermodynamic modelling; Modified quasichemical model; Al–Ca–Sr system

1. Introduction

The Al–Ca–Sr ternary system is an important subsystem in the family of creep resistant Mg–Al–Ca–Sr alloys [1,2]. Therefore, accurately assessing the thermodynamics and phase stability in Al–Ca, Ca–Sr, and Al–Sr binary systems is important for developing a reliable thermodynamic database of Mg-alloys as well as Al-alloys. To create an accurate thermodynamic model of a ternary system, it is necessary to have thermodynamic descriptions of the three constituent binary systems first. In order to provide a good prediction for the thermodynamic properties of the Al–Ca–Sr system, it is necessary to use the suitable model that describes the excess Gibbs free energy. If a model based on random mixing is used for the liquid phase, higher order interaction parameters are needed to reproduce the *liquidus* around the intermetallic compounds and it often results in a less satisfactory *liquidus* at other compositions. In the Al–Ca system, the measured heat of mixing forms a V-shape with a minimum around 0.4 at.% Ca, which indicates a tendency for short-range ordering. Furthermore, according to You *et al.* [3], there is a strong evidence for the existence of molecular, such as Al_2Ca, species that are called associates, in the liquid phase. To deal with short range ordering, the associates model was proposed in the literature. However, this model is not physically sound, since it assumes that some molecules occupy specific atomic positions. Furthermore, using a random solution model to treat liquids with short range ordering continues to appear in the literature. In reality, a random solution model is only expected at very high temperature when the entropy term overwhelms any tendency for ordering or clustering of atoms. It follows that the configurational entropy of mixing should vary with temperature. The modified quasichemical solution model provides a better treatment of configurational entropy that accounts for a non-random distribution of atoms. Therefore, models based on the random mixing can not properly describe the influence of short-range ordering, as they do not solve the problem of the configurational entropy. The description of short-range ordering can be taken into account with bond energy models by considering the interactions between atoms that extend beyond the nearest neighbours approximation. This problem has been treated

* Corresponding author. Tel.: +1 514 848 2424x3146; fax: +1 514 848 3175.
E-mail address: mmedraj@encs.concordia.ca (M. Medraj).
URL: http://www.me.concordia.ca/~mmedraj (M. Medraj).

0021-9614/$ - see front matter © 2007 Elsevier Ltd. All rights reserved.
doi:10.1016/j.jct.2007.10.003

using the modified quasichemical model [4,5]. The model is the so-called because it has a mass-action equation that is typical in chemical reaction theory.

No information on phase equilibria, ternary compounds, or experimental thermodynamic data for the Al–Ca–Sr ternary system could be found in the literature, thus this work was initiated to evaluate critically the thermodynamic description of this system using the modified quasichemical model.

2. Experimental data

2.1. Al–Sr system

According to Burylev *et al.* [6], Vakhobov *et al.* [7], and Vakhobov *et al.* [8], the assessed phase diagram of the Al–Sr system consists of liquid, Sr-fcc and Sr-bcc, Al_4Sr, Al_2Sr, Al_7Sr_8, and terminal solid solution, Al-fcc, with a low solubility of 0.6 at.% Sr at $T = 773.15$ K after annealing for a period of 450 h [8]. Vakhobov *et al.* [8] reported that Sr dissolved 5.0 at.% Al at $T = 873.15$ K, whereas Closset *et al.* [13] found a negligible solid solubility in this system. Furthermore, comparing the mutual solubility between Al and Sr with a similar system such as Al–Ca, the most reliable measurements show very low solubility of Ca in Al. Moreover, in view of the relative atomic radii of Al and Sr atoms, the ratio of Al radius to that of Sr is 0.67 indicating the chance for low solid solubility. Therefore, the experimental solubility of [8] is not considered reliable. In this work, it is assumed that the mutual solubility of the components in Al–Sr system is negligible. The intermetallic compound Al_3Sr_8 was predicted using first-principle calculations by Wolverton *et al.* [9] based on the existence of the Al_3Ca_8 compound in the Al–Ca system [10,11].

Over a complete composition range using differential thermal analysis (DTA), the Al–Sr system was investigated by Burylev *et al.* [6] and Vakhobov *et al.* [7,8]. Whereas, Bruzzone and Merlo [12] studied this system by thermal analysis, X-ray diffraction (XRD), and metallographic methods, the starting materials were 99.8 wt% Sr and 99.99 wt% Al. They reported that Al_4Sr melts congruently at $T = 1313.15$ K. However, Burylev *et al.* [6] and Closset *et al.* [13] reported this melting point as $T = (1273.15 \pm 20)$ and $T = 1298.15$ K, respectively. In addition, Al_2Sr melts congruently at $T = 1209.15$ K according to [12] compared to Closset's [13] result at $T = 1193.15$ K. Furthermore, Bruzzone and Merlo [12] concluded that Al_7Sr_8 decomposes by peritectic reaction at $T = 939.15$ K.

Sato *et al.* [14] studied the Al-rich region of the Al–Sr system using thermal analysis, XRD and optical microscopy. They reported that the invariant reaction in Al-rich region occurs at 0.85 at.% Sr and $T = 927.15 \pm 1$ K, compared to the results of Closset *et al.* [13] as 0.75 at.% Sr and $T = 927.15$ K. Whereas, Hanna and Hellawell's [15] values are 1.3 at.% Sr and $T = 926.15$ K. Closset *et al.* [13] and Burylev *et al.* [6] reported that the eutectic reaction in the Sr-rich region occurs at $T = 853.15$ K and 73.5 at.% Sr, and at $T = 833.15$ K and ~70 at.% Sr, respectively. Closset *et al.* [13] mentioned that they had difficulties with detection of the thermal arrests in the alloys containing more than 60 at.% Sr. Therefore, the *liquidus* points at higher Sr concentrations seem to be less reliable than that in the work of Bruzzone and Merlo [12].

Alcock and Itkin [16] first reviewed and optimised the Al–Sr system. Subsequently, several efforts [17–20] have been made to calculate this system. The Al–Sr phase diagram presented by Chartrand and Pelton [17] is different from that published by Alcock and Itkin [16], especially in the Sr-rich part. The calculated phase diagram agrees reasonably well with most of the experimental data except for the melting behaviour of Al_2Sr. The calculations of the Al–Sr phase diagram [16,18,19] show that Al_2Sr melts incongruently because of symmetry in the Al_4Sr *liquidus*. In contrast, the interpretations of the experimental data of Closset *et al.* [13], and Bruzzone and Merlo [12] showed asymmetry in Al_4Sr *liquidus* and congruent melting of Al_2Sr which is in agreement with Chartrand and Pelton's [17] assessment. In this work, therefore, melting of the intermetallic compound Al_2Sr is considered to be congruent.

Sommer *et al.* [20] and Esin *et al.* [21] measured the enthalpy of mixing of the Al–Sr liquid at $T = (1070.15, 1125.15, 1130.15, 1173.15,$ and $1175.15)$ K, using a high temperature mixing calorimeter. Burylev *et al.* [6] and Vakhobov *et al.* [7] measured the vapour pressure of Sr over the temperature range of (1123.15 to 1373.15) K using the Knudsen effusion method. Based on these data, they [6,7] derived the activities of Sr in Al–Sr liquid. Srikanth and Jacob [23] measured the activity of Sr in Al–Sr liquid at $T = 1323.15$ K in the composition range less than 17 at.% Sr and greater than 28 at.% Sr using Knudsen effusion-mass loss technique and pseudo isopiestic technique, respectively. These data are employed in the current work.

2.2. Al–Ca system

In 1908, Donski [24] carried out the first attempt to construct the Al–Ca system using thermal analysis. This led Matsuyama [25] to investigate the Al–Ca system by thermal analysis, electrical resistance and microscopic examination. His samples were prepared from 99.4 wt% Al and 98.34 wt% Ca. He determined the *liquidus* line, two eutectic reactions; one in the Al-rich region occurring at 5.2 at.% Ca and $T = 889.15$ K, compared to Donski's [24] results as 5.5 at.% Ca and $T = 883.15$ K. Whereas, Kevorkov and Schmid-Fetzer's [11] values are 5.1 at.% Ca and $T = 886.15$ K. The other eutectic is in the Ca-rich side and according to Matsuyama [25], it occurs at 64.5 at.% Ca and $T = 818.15$ K, compared to Donski's [24] values as 66.9 at.% Ca and $T = 823.15$ K, and Kevorkov and Schmid-Fetzer's [11] results as 66.3 at.% Ca and $T = 829.15$ K. These results will be used for comparison with the current assessment.

In the Al–Ca system, most of the experimental investigations deal mainly with the Al-rich corner, which is technically interesting for aluminium alloys. Nevertheless, Kevorkov and Schmid-Fetzer [11] investigated the entire Al–Ca system using X-ray diffraction, SEM/EDX analysis, metallographic, and diffusion couple techniques. They [11] reported four intermetallic compounds; Al_2Ca which melts congruently at $T = 1359.15$ K compared to Matsuyama's [25] value at $T = 1352.15$ K, Al_3Ca_8 which melts congruently at $T = 852.15$ K, Al_4Ca which decomposes at $T = 973.15$ K compared to Donski's [24] and Matsuyama's [25] values at $T = 963.15$ and $T = 973.15$ K, and AlCa which melts incongruently at $T = 906.15$ K. However, Huang and Corbett [10] reported, also, the occurrence of $Al_{14}Ca_{13}$ compound with monoclinic structure instead of AlCa. Nowotny *et al.* [26] determined the crystal structure of Al_4Ca and Al_2Ca as bct and fcc, respectively. Huang and Corbett [10] investigated the crystal structures of $Al_{14}Ca_{13}$ and Al_3Ca_8 using X-ray analysis and noted that they have monoclinic and triclinic structures, respectively.

Several researchers [25,27–30] measured the solubility of Ca in Al. Among them Edwards and Taylor [29] and Jaquet and Warlimont [30] reported negligible solubility and their results agree fairly well. Therefore, the mutual solubility of the components in Al–Ca system is considered negligible in this work.

The enthalpy of formation of Al_2Ca and Al_4Ca compounds was measured by many researchers [31–36]. Notin *et al.* [31,32] determined the enthalpy of formation of these compounds at $T = 953.15$ K and $T = 1038.15$ K precisely. They recorded calorimetric signals that corresponded to the enthalpy change during the addition of a solid Ca to the Al melt. There is a reasonable agreement with the values of enthalpy of formation for Al_2Ca between [32,36]. According to Kevorkov *et al.* [36], the small difference between them may be due to the difference in heat capacity, ΔC_p, for the formation reaction between room temperature and $T = 1038.15$ K. There are no experimental data on the enthalpy of formation of the $Al_{14}Ca_{13}$ intermetallic compound reported in the literature up to date and according to Kevorkov *et al.* [36]. This is due to the sluggish formation kinetics of the phase and thus difficulty of preparing an $Al_{14}Ca_{13}$-rich sample. The enthalpy of formation of the Al_3Ca_8 phase was measured using drop solution calorimetry by Kevorkov *et al.* [36].

Notin *et al.* [32], Sommer *et al.* [20], and Kevorkov *et al.* [36] measured the heat of mixing of liquid Al–Ca alloys. Their experimental results are in good agreement. Jacob *et al.* [37] determined the activity of the components in the Al–Ca liquid using Knudsen effusion method for alloys in the composition range less than 38 at.% and greater than 44 at.% Ca at $T = 1373$ K. Schürmann *et al.* [38] measured the activities of Ca in the liquid alloys using boiling point determination technique. The activity measurements by Jacob *et al.* [37] and Schürmann *et al.* [38] agree fairly well.

Kevorkov and Schmid-Fetzer [11] calculated the phase diagram of the Al–Ca system using the random solution model. In order to adjust the *liquidus* around Al_2Ca, their calculated enthalpy of mixing deviated from the experimental data, whereas fitting the enthalpy of mixing to the experimental data resulted in shifting the *liquidus* line of Al_2Ca to a higher temperature. When the random solution model is used for the liquid, higher order interaction parameters in the liquid are needed to reproduce the *liquidus* around Al_2Ca and it often results in less satisfactory *liquidus* at other compositions. Ozturk *et al.* [39] used both random and associate model to re-optimise the Al–Ca system. They found that while the random solution model gives better agreement with the experimental phase diagram, the associate model agrees well with the experimental thermodynamic data.

2.3. Ca–Sr system

Several researchers [40–47] studied the Ca–Sr phase diagram. Among them Schottmiller *et al.* [40] determined the *liquidus* and *solidus* lines by thermal analysis with ±6 K uncertainty. They prepared Ca–Sr alloys from 99.8 wt.% Ca and 99.7 wt.% Sr in an iron crucible under an argon atmosphere. Schottmiller *et al.* [40] reported that the *liquidus* line has a minimum at 62 at.% Sr and $T = 1011.15$ K, and there are three allotropies of Ca and Sr. According to Peterson and Fattore [44], however, this is due to the hydrogen contamination in the Ca and Sr samples. A more reliable work by Smith *et al.* [43] stated that there are only two allotropies occurring in both pure Ca and Sr.

Mutual solubility between Ca and Sr throughout the entire composition range is considered in the current work. Both pure Ca and Sr have the same type of allotropic phase transformation from fcc to bcc at $T = 716.15$ K and $T = 829.15$ K [41], respectively.

Predel and Sommer [48] measured the enthalpy of mixing of the Ca–Sr liquid at $T = 1143.15$ K using high temperature calorimetry. The excess entropy of mixing of the Ca–Sr liquid is assumed to be zero by Predel and Sommer [48].

2.4. Al–Ca–Sr system

No data describing the experimental thermodynamic or phase equilibrium for the Al–Ca–Sr ternary system could be found in the literature. Thus, this work was initiated to evaluate critically the thermodynamic description of this system using the modified quasichemical model. The phase equilibria will be established for this system based on the optimised binary subsystems.

3. Thermodynamic models

For a pure element with a certain structure ϕ, its Gibbs free energy, referenced at room temperature, is described as

$$^{\circ}G_A^{\varphi} = a + b(T/\mathrm{K}) + c(T/\mathrm{K})ln(T/\mathrm{K}) + d(T/\mathrm{K})^2 + e(T/\mathrm{K})^3 + f(T/\mathrm{K})^{-1} + g(T/\mathrm{K})^7 + h(T/\mathrm{K})^{-9}, \quad (1)$$

where the parameters a to h are assigned from the SGTE database [49].

The Gibbs free energy function of the stoichiometric compound is represented by equation (2):

$$G^{\text{phase},\varphi} = x_i^{\circ}G_i^{\varphi} + x_j^{\circ}G_j^{\varphi} + \Delta G_f, \tag{2}$$

where ${}^{\circ}G_i^{\varphi}$ and ${}^{\circ}G_j^{\varphi}$ denote the Gibbs free energy of element i and j in their standard state and $\Delta G_f = a + b(T/\text{K})$ represents the Gibbs free energy of formation of the stoichiometric compound, where a and b are the model parameters to be optimised using experimental data.

The Gibbs free energy of a disordered solution phase is described by the following equation:

$$G = x_i^{\circ}G_i^{\Phi} + x_j^{\circ}G_j^{\Phi} + R(T/\text{K})[x_i \ln x_i + x_j \ln x_j] + {}^{\text{ex}}G^{\phi}, \tag{3}$$

where Φ denotes the phase in question and x_i, x_j denote the mole fraction of component i and j, respectively. The excess Gibbs free energy of a disordered solution is represented using the Redlich–Kister equation:

$$\begin{aligned} &{}^{\text{ex}}G^{\Phi} = x_i.x_j \sum_{n=0}^{n=m} {}^{n}L_{i,j}^{\phi}(x_i - x_j)^n, \\ &\text{with } {}^{n}L_{i,j}^{\phi} = a_n + b_n \times T \quad (n = 0, \ldots, m), \end{aligned} \tag{4}$$

where ${}^{n}L_{i,j}^{\Phi}$ is the interaction parameters, a_n and b_n are model parameters to be optimised in terms of experimental phase diagram and thermodynamic data.

In this study, two complete solid solutions, fcc and bcc, were modelled in the Ca–Sr system using the random solution model described in equations (3) and (4).

The molar Gibbs free energy for the liquid phase, derived from quasichemical theory [50], is described by the following equation:

$$G^{\text{liq}} = n_i^{\circ}G_i^{\text{liq}} + n_j^{\circ}G_j^{\text{liq}} - T\Delta S^{\text{config}} + \frac{n_{ij}}{2}\Delta^{\text{exs}}G^{\text{liq}}, \tag{5}$$

where n_i and n_j are the number of moles of the component i and j, n_{ij} is the number of (i–j) pairs, ΔS^{config} is the configurational entropy of mixing given for randomly distributing the (i–i), (j–j), and (i–j) pairs:

$$\begin{aligned} \Delta S^{\text{config}} = -R[n_i \ln(x_i) + n_j \ln(x_j)] - R\Bigg[n_{ii} \ln\left(\frac{x_{ii}}{y_i^2}\right) + \\ n_{jj} \ln\left(\frac{x_{jj}}{y_j^2}\right) + n_{ij} \ln\left(\frac{x_{ij}}{2y_iy_j}\right)\Bigg], \end{aligned} \tag{6}$$

where x_i and x_j are the overall mole fractions of the components i and j, respectively,

$$x_i = \frac{n_i}{n_i + n_j}, \tag{7}$$

$$\text{Pair fraction}: \quad x_{ii} = \frac{n_{ii}}{n_{ii} + n_{jj} + n_{ij}}, \tag{8}$$

and the coordination-equivalent fractions :

$$y_i = \frac{Z_i n_i}{Z_i n_i + Z_j n_j}, \tag{9}$$

where Z is the coordination number.

The mass balance in the quasichemical model gives [51]

$$Z_i n_i = 2n_{ii} + n_{ij}, \tag{10}$$

$$Z_j n_j = 2n_{jj} + n_{ij}. \tag{11}$$

Substitution of equations (10) and (11) into equations (8) and (9) gives

$$\begin{aligned} y_i &= x_{ii} + \frac{x_{ij}}{2}, \\ y_j &= x_{jj} + \frac{x_{ij}}{2} \end{aligned} \tag{12}$$

The expansion of ${}^{\text{ex}}G^{\text{liq}}$ as a polynomial in terms of the pair fraction x_{ii}, x_{jj}, x_{ij} is represented by the following equation (13) [5]:

$$\Delta^{\text{ex}}G^{\text{liq}} = \Delta g_{ij}^{\circ} + \sum_{\substack{i\geqslant 1 \\ m\geqslant 1}} g_{ij}^{m\circ}x_{ii}^{m} + \sum_{\substack{j\geqslant 1 \\ n\geqslant 1}} g_{ij}^{\circ n}x_{ij}^{n}. \tag{13}$$

The parameters, Δg_{ij}°, $g_{ij}^{i\circ}$ and $g_{ij}^{\circ j}$ are to be optimised using experimental data.

Chartrand and Pelton [4] modified the quasichemical model, in order to permit the coordination number to vary with compositions, as follows:

$$\begin{aligned} \frac{1}{Z_i} &= \frac{1}{Z_{ii}^{i}}\left(\frac{2n_{ii}}{2n_{ii} + n_{ij}}\right) + \frac{1}{Z_{ij}^{i}}\left(\frac{n_{ij}}{2n_{ii} + n_{ij}}\right), \\ \frac{1}{Z_j} &= \frac{1}{Z_{jj}^{j}}\left(\frac{2n_{jj}}{2n_{jj} + n_{ij}}\right) + \frac{1}{Z_{ji}^{j}}\left(\frac{n_{ij}}{2n_{jj} + n_{ij}}\right), \end{aligned} \tag{14}$$

where Z_{ii}^{i} and Z_{ij}^{i} are the values of the coordination number of the ith atom when all nearest neighbours are i's and j's, respectively.

Substituting equation (14) in equations (10) and (11) gives

$$\begin{aligned} n_i &= \frac{2n_{ii}}{Z_{ii}^{i}} + \frac{n_{ij}}{Z_{ij}^{i}}, \\ n_j &= \frac{2n_{jj}}{Z_{jj}^{i}} + \frac{n_{ij}}{Z_{ji}^{i}}. \end{aligned} \tag{15}$$

The coordination number of the pure elements in the metallic liquid solution, $Z_{\text{CaCa}}^{\text{Ca}} = Z_{\text{AlAl}}^{\text{Al}} = Z_{\text{SrSr}}^{\text{Sr}}$, is set to be 6 which is the same coordination number used by Pelton and Chartrand [4]. The coordination number of the pairs; $Z_{\text{AlCa}}^{\text{Al}}$,$Z_{\text{CaAl}}^{\text{Ca}}$,$Z_{\text{AlSr}}^{\text{Sr}}$,$Z_{\text{SrAl}}^{\text{Al}}$, $Z_{\text{CaSr}}^{\text{Sr}}$, and $Z_{\text{SrCa}}^{\text{Ca}}$ are chosen to permit the composition of maximum short range ordering in the binary system to be consistent with the composition that corresponds to the minimum heat of mixing. The tendency to maximum short range ordering near the composition 40 at.% Ca in the Al–Ca system was obtained by setting $Z_{\text{AlCa}}^{\text{Al}} = 6$ and $Z_{\text{CaAl}}^{\text{Ca}} = 4$. In the Al–Sr system, the tendency to maximum short range ordering near the composition 40 at.% Sr was obtained by setting $Z_{\text{AlSr}}^{\text{Sr}} = 4$ and $Z_{\text{SrAl}}^{\text{Al}} = 6$. The positive heat of mixing in Ca–Sr system reflects the fact that formation of Ca–Ca and Sr–Sr pairs is

more favourable than formation of Ca–Sr pairs. This indicates that the coordination number for Ca–Sr pairs should be small. Hence the parameters Z^{Sr}_{CaSr} and Z^{Ca}_{SrCa} are set to be 3 in this work.

Thermodynamic optimisation and calculations were performed in this work using FactSage program [52].

4. Results and discussion

4.1. Al–Sr system

The re-optimised Al–Sr system along with all experimental data from the literature is shown in figure 1. As can be seen from this figure, the calculated *liquidus* and invariant points are in good agreement with the experimental data of Closset *et al.* [13], and Bruzzone and Merlo [12] but differ slightly from those obtained by Vakhobov *et al.* [7] and Vakhobov *et al.* [8]. The results of Closset *et al.* [13] are supported with a good description of the experimental methods and they are considered more reliable compared to [7,8] works which are in agreement with Chartrand and Pelton's [17] assessment. Table 1 lists the thermodynamic model parameters obtained by optimisation using the experimental thermodynamic and phase equilibrium data from the literature. The calculated invariant points in relation to the experimental data from the literature are presented in table 2. The calculated *liquidus* and invariant points of the Al–Sr system are in good agreement with the experimental data up to 60 at.% Sr as can be seen in table 2 and figure 1. It is noteworthy that discrepancies between the calculated and experimental data in the Sr-rich region are due to the high reactivity of Sr. In addition, the experimental phase diagram shows uncertainties for the *liquidus* and invariant points in the Sr-rich region.

The calculated heat of mixing of Al–Sr liquid at $T = 1125.15$ K is plotted in figure 2 together with experimental values from the literature [20,21]. As can be seen in this figure, the calculated heat of mixing of Al–Sr liquid

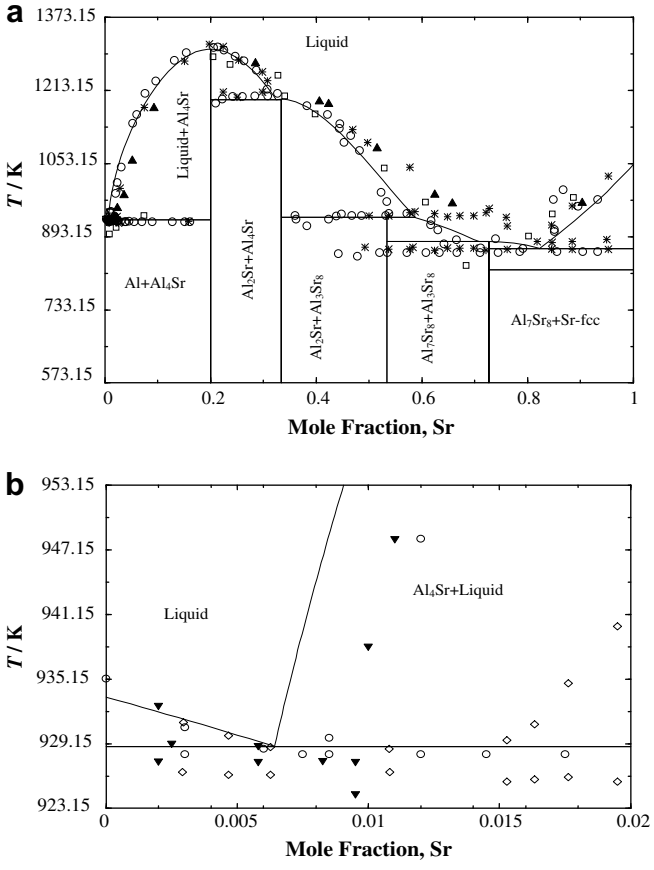

FIGURE 1. (a) Re-optimised phase diagram for the Al–Sr system, (b) Al-rich region of the Al–Sr system: ○: [13]; ✳ [12]; ▲: [8]; □: [22]; ▼: [14]; ◇: [15].

TABLE 1
Optimised thermodynamic parameters of the Al–Ca, Al–Sr, and Ca–Sr systems in $J \cdot mol^{-1} \cdot atom^{-1}$

Liquid (Al,Ca)	$\Delta^{ex}G^{liq} = -1296.4 + 0.48(T/K) + \{-0.142(T/K)\}x_{Ca,Ca} + \{134.3 + 0.031(T/K)\}x_{Al,Al}$ $Z^{Al}_{AlCa} = 6$ $Z^{Ca}_{CaAl} = 4$
Liquid (Al,Sr)	$\Delta^{ex}G^{liq} = -1511.5 + 0.54(T/K) + \{-187.10 - 0.269(T/K)\}x_{Sr,Sr} + \{442.76 - 0.108(T/K)\}x_{Al,Al}$ $Z^{Sr}_{AlSr} = 4$ $Z^{Al}_{SrAl} = 6$
Liquid (Ca,Sr)	$\Delta^{ex}G^{liq} = 43.74 + 0.01(T/K) + 22.85x_{Ca,Ca} - 6.09x_{Sr,Sr}$ $Z^{Sr}_{CaSr} = 3$ $Z^{Ca}_{SrCa} = 3$
Al_2Ca	$G^{Al_2Ca}_{Al:Ca} = -28559 + 1.8(T/K)$
Al_4Ca	$G^{Al_4Ca}_{Al:Ca} = -17327 + 0.46(T/K)$
Al_3Ca_8	$G^{Al_3Ca_8}_{Al:Ca} = -16309 + 0.21(T/K)$
$Al_{14}Ca_{13}$	$G^{Al_{14}Ca_{13}}_{Al:Ca} = -28209 + 0.18(T/K)$
Al_4Sr	$G^{Al_4Sr}_{Al:Sr} = -30853 + 1.4(T/K)$
Al_3Sr_8	$G^{Al_3Sr_8}_{Al:Sr} = -11868 + 0.4(T/K)$
Al_7Sr_8	$G^{Al_7Sr_8}_{Al:Sr} = -21198 + 0.25(T/K)$
Al_2Sr	$G^{Al_2Sr}_{Al:Sr} = -30409 + 2.1(T/K)$
bcc	$G^{bcc}_{Ca:Sr} = 3770.0 + 0.01(T/K)$
fcc	$G^{fcc}_{Ca:Sr} = 3770.0 + 0.11(T/K)$

Standard state of the liquid phase is liquid component; standard state of the stoichiometric compounds is solid.

TABLE 2
Comparison between calculated and experimental values of the invariant reactions in the Al–Sr system

Reaction	at.% Al	at.% Sr	T/K	Reference	Reaction type
$L \leftrightarrow Al + Al_4Sr$	99.25	0.75	927.15	[13]	Eutectic
	99.15	0.85	927.15 ± 1	[14]	
	98.70	1.30	926.15	[15]	
	99.36	0.64	929.15	[This work]	
$L \leftrightarrow Al_4Sr$	80.00	20.00	1273.15 ± 20	[6]	Congruent
	80.00	20.00	1313.15	[12]	
	80.00	20.00	1298.15	[13]	
	80.00	20.00	1311.15	[8]	
	80.00	20.00	1302.15	[This work]	
$L + Al_4Sr \leftrightarrow Al_2Sr$	66.67	33.33	1209.15	[12]	Peritectic
	66.67	33.33	1193.15	[13]	
	66.67	33.33	1196.15	[This work]	
$L + Al_2Sr \leftrightarrow Al_7Sr_8$	46.67	53.33	939.15	[12]	Peritectic
	46.67	53.33	937.15	[13]	
	46.67	53.33	940.15	[This work]	
$L \leftrightarrow$ Sr-bcc	0.00	100.00	1042.15	[40]	Melting
	0.00	100.00	1043.15	[This work]	
$L \leftrightarrow Al_7Sr_8 + Al_3Sr_8$	27.50	72.50	866.15	[12]	Eutectic
	27.29	72.71	877.15	[This work]	
$L \leftrightarrow$ Sr-bcc $+ Al_3Sr_8$	19.22	80.78	872.15	[This work]	Eutectic

agrees well with the experimental data. The reported data are consistent over the entire composition range and show no temperature dependence. Figure 2 shows that the minimum value of the heat of mixing occurs around 40 at.% Sr which indicates high stability of the liquid and a tendency for short range ordering. The experimentally measured Sr activity in the liquid phase [6,7,23] is compared with the calculation performed at $T = 1323.15$ K as shown in figure 3. It can be seen in this figure that mixing up to 60 at.% of Sr in the Al–Sr liquid demonstrates negative deviation from Raoult's ideal solution, but mixing 60–100 at.% Sr in the liquid obeys Raoult's model for the ideal solution.

4.2. Al–Ca system

The experimental phase diagram, enthalpy of mixing, and the activities of Al and Ca in the liquid phase were used to optimise the thermodynamic model parameters of the liquid and the intermetallic compounds in this system. The optimised model parameters as well as the binary invariant points are given in tables 1 and 3, respectively.

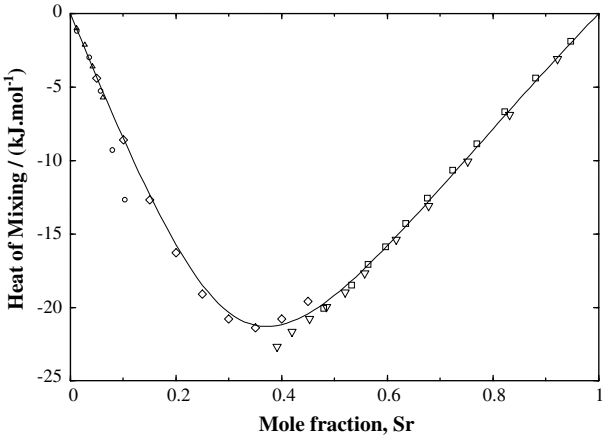

FIGURE 2. Plot of the calculated heat of mixing against mole fraction Sr for the Al–Sr liquid at $T = 1125.15$ K. ○: 1130.15 K [20], □: 1070.15 K [20]; △: 1125.15 K [20]; ▽: 1175.15 K [20]; ◇: 1173.15 K [21]. (Reference state: Al-liquid and Sr-liquid).

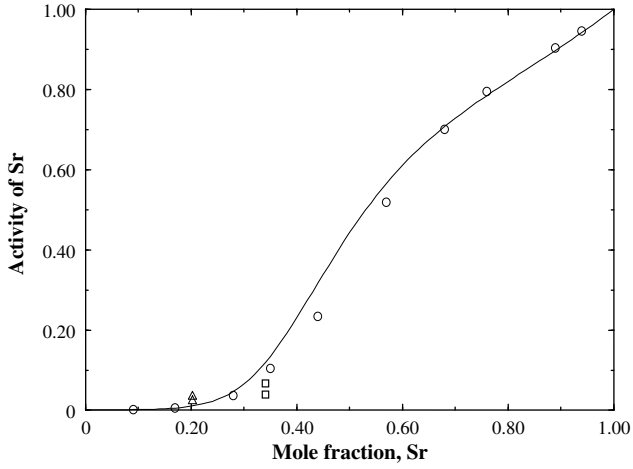

FIGURE 3. Plot of calculated activity of Sr against mole fraction Sr for the Al–Sr liquid at $T = 1323.15$ K. △: 1123.15–1373.15 K [6], ○: 1323.15 K [23], □: 1123.15–1373.15 K [7]. (Reference state: Al-liquid and Sr-liquid).

TABLE 3
Comparison between calculated and experimental values of the invariant reactions in the Al–Ca system

Reaction	at.% Al	at.% Ca	T/K	Reference	Reaction type
L ↔ Al-fcc	100.00	0.00	934.15	[40]	Melting
	100.00	0.00	934.15	This work	
L ↔ Al-fcc + Al_4Ca	94.90	5.10	886.15	[11]	Eutectic
	94.80	5.20	889.15	[25]	
	94.50	5.50	883.15	[24]	
	95.22	4.78	885.15	This work	
L + Al_2Ca ↔ Al_4Ca	80.00	20.00	963.15	[24]	Peritectic
	80.00	20.00	973.15	[25]	
	80.00	20.00	973.15	[11]	
	80.00	20.00	973.15	This work	
L ↔ Al_2Ca	66.67	33.33	1352.15	[25]	Congruent
	66.67	33.33	1359.15	[11]	
	66.67	33.33	1356.15	This work	
L + Al_2Ca ↔ $Al_{14}Ca_{13}$	50.00	50.00	906.15	[11]	Peritectic
	51.85	48.15	904.15	This work	
L ↔ $Al_{14}Ca_{13}$+Al_3Ca_8	35.50	64.50	818.15	[25]	Eutectic
	33.70	66.30	829.15	[11]	
	33.10	66.90	823.15	[24]	
	33.44	66.56	830.15	This work	
L ↔ Ca-bcc+Al_3Ca_8	20.00	80.00	833.15	[11]	Eutectic
	20.44	79.56	827.15	This work	
L ↔ Al_3Ca_8	27.27	72.73	852.15	[11]	Congruent
	27.27	72.73	843.15	This work	

The re-optimised phase diagram of the Al–Ca system in relation to the experimental data from the literature is shown in figure 4. Good agreement between the re-optimised phase diagram and the measured *liquidus* points of [11,24,25] can be observed in this figure.

The calculated enthalpy of mixing at $T = 1100.15$ K and the experimental data of Sommer *et al.* [20] and Notin *et al.* [31] are shown in figure 5. As can be seen from this figure, the calculated heat of mixing of liquid Al–Ca is in good agreement with the experimental data. The calculated entropy of mixing of the Al–Ca liquid at $T = 1100.15$ K shows a minimum value near the 35 at.% Ca composition which corresponds to the composition where the enthalpy of mixing is minimum indicating a tendency for short range ordering in the Al–Ca liquid as can be seen in figure 6. Figures 7 and 8 show the calculated activities of Al and Ca in the Al–Ca liquid at $T = 1373.15$ K along with the experimental data of Jacob *et al.* [37] and Schürmann *et al.* [38]. The calculated activities show good agreement with the experimental data. The

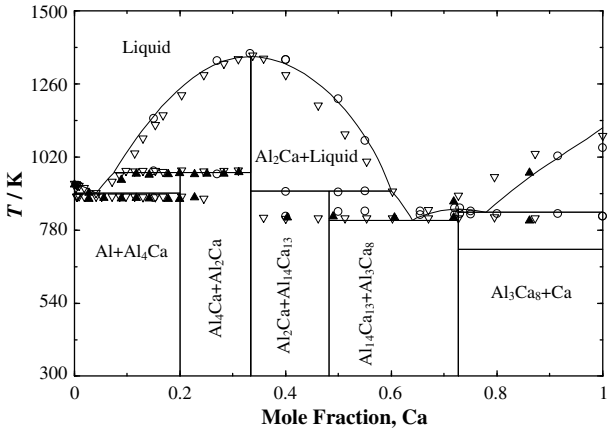

FIGURE 4. Re-optimised phase diagram for the Al–Ca system. ○: [11]; ▽: [25]; ▲: [24].

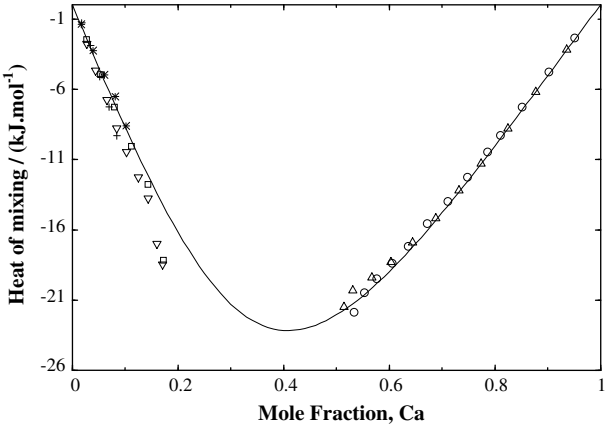

FIGURE 5. Plot of the calculated heat of mixing against mole fraction of Ca for the Al–Ca liquid against at $T = 1100$ K. ○: 1130.15 K [20]; □: 1070.15 K [20]; △: 1125.15 K [20]; ▽: 1175.15 K [20]; ∗: 1173.15 K [21]. (Reference state: Al-liquid and Ca-liquid).

calculated heat of formation of the intermetallic compounds in the Al–Ca system along with the measured heat of formation is plotted in figure 9. The calculated and the measured heat of formation of the compounds in the Al–Ca system are in accord.

4.3. Ca–Sr system

Figure 10 shows the calculated Ca–Sr phase diagram in relation to the experimental data of Schottmiller *et al.* [40], and Predel and Sommer [48]. The re-optimised Ca–Sr system agrees well with the experimental data. The data of the heat of mixing by Predel and Sommer [48] were used in the optimisation and matched the calculated heat of mixing curve seen in figure 11. Physically, the heat of mixing is positive reflecting the fact that formation of Ca–Ca and Sr–Sr pairs is more favourable than formation of Ca–Sr pairs. In this work, the excess entropy of mixing of the liquid alloys is relatively small with maximum value of

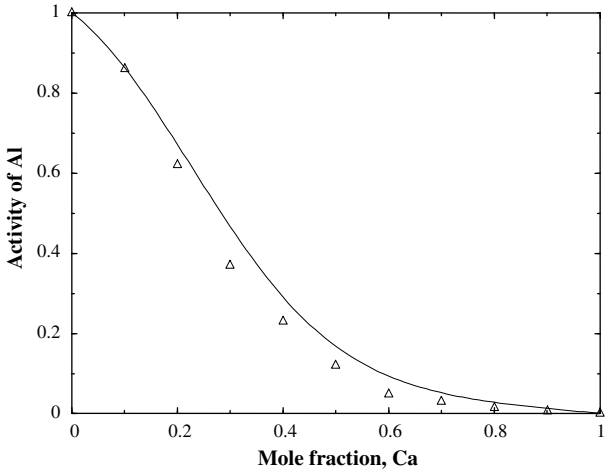

FIGURE 8. Plot of calculated activity of Al against mole fraction Ca for in the Al–Ca liquid at $T = 1373.15$ K. △: 1373.15 K [37]. (Reference state: Al-liquid, Ca-liquid).

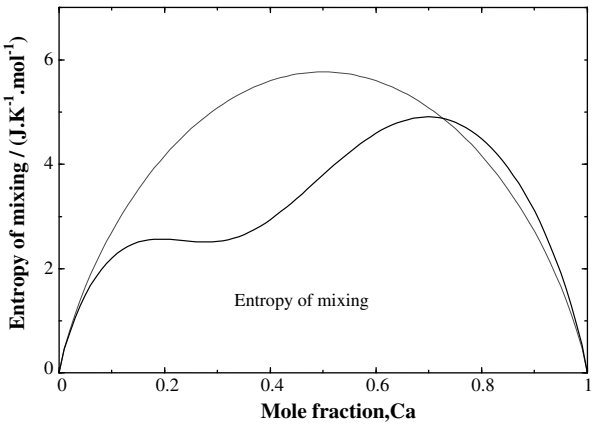

FIGURE 6. Plot of the entropy of mixing of the Al–Ca liquid at $T = 1100.15$ K (- - - - - ideal; ——, actual).

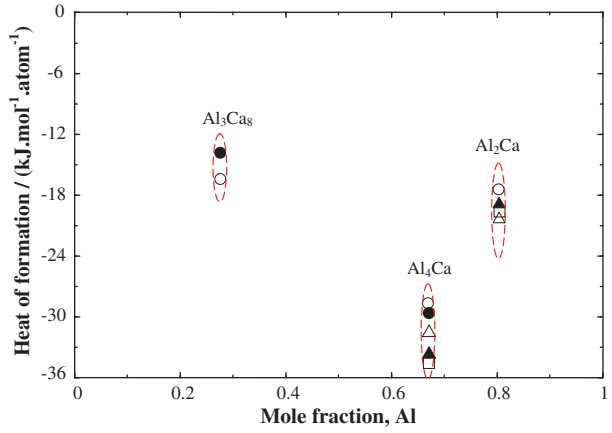

FIGURE 9. Plot of heat of formation against mole fraction Al for different intermetallic compounds in the Al–Ca system. ○: 298 K [this work]; △: 673–903 K [33]; ▲: 1038 K [31]; □: 800 K [32]; ●: 298 K [36].

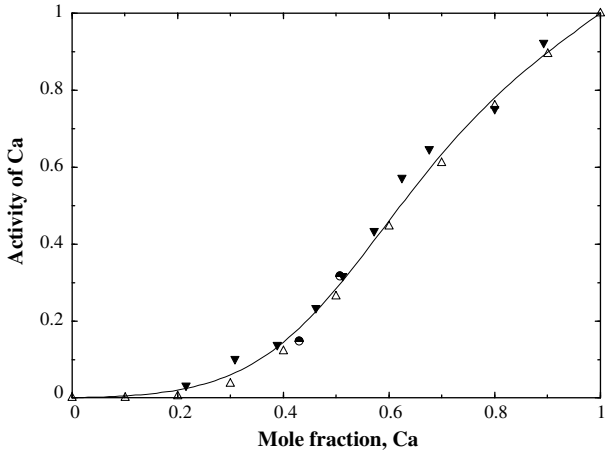

FIGURE 7. Plot of the calculated activity of Ca against mole fraction Ca for the Al–Ca liquid at $T = 1373.15$ K, △: 1373.15 K [37]; ▼: 1630.15 K [38], ◓: 1480.15 K [38]. (Reference state: Al-liquid, Ca-liquid).

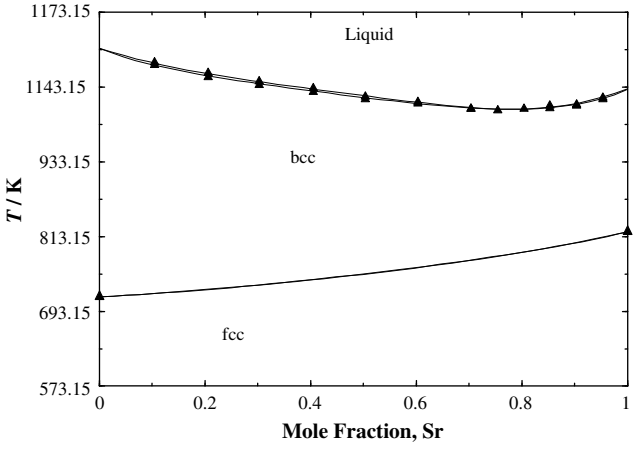

FIGURE 10. Plot of temperature against mole fraction Sr for the re-optimised Ca–Sr system. ▲: [40].

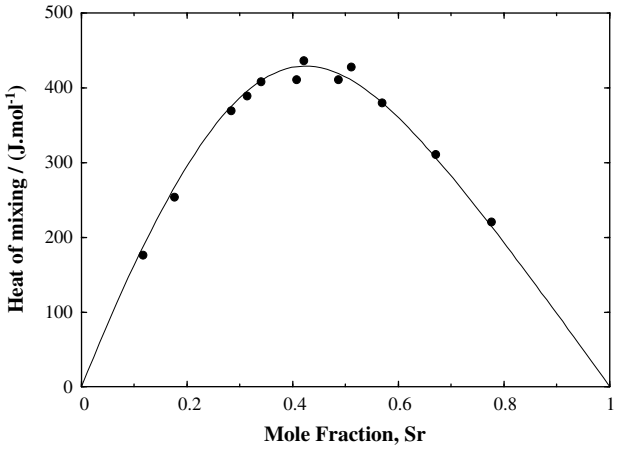

FIGURE 11. Plot of the calculated heat of mixing against mole fraction Sr for the Ca–Sr liquid at $T = 1143.15$ K. ●: [48] (Reference state: Ca-liquid, Sr-liquid).

$+0.02\ \mathrm{J \cdot mol^{-1} \cdot K^{-1}}$ which is in agreement with the evaluation of Alcock *et al.* [47].

Due to the lack of experimental thermodynamic data for the Ca–Sr system, its thermodynamic description was predicted based on the experimental work of Schottmiller *et al.* [40] and Predel and Sommer [48] only.

4.4. Al–Ca–Sr system

The thermodynamic properties of the liquid were estimated from the optimised binary parameters using the Toop extrapolation [53]. This is an asymmetric extrapolation method that is used in this work because Ca and Sr have similar properties which are different from those of Al. For this purpose, Ca and Sr were placed in the same group while Al was in a different group. No ternary adjustable terms were added since experimental thermodynamic data for the Al–Ca–Sr system could not be found in the literature. The database was then used to calculate polythermic projections of the *liquidus* surfaces shown in figures 12 and 13. The Al–Ca–Sr ternary system is presented as a projection using the Gibbs triangle at various temperatures and constant pressure. The calculated *liquidus* projection, as can be seen in figures 12 and 13, is divided into 11 primary crystallization fields: Al_4Sr, Al_2Sr, Al_3Sr_8, Al_7Sr_8, Al_2Ca, Al_4Ca, Al_3Ca_8, $Al_{14}Ca_{13}$, Al, fcc, and bcc. The model predicted one saddle point, one peritectic, seven quasi-peritectics, and two ternary eutectics. The respective reactions of these points are listed in table 4.

In view of the fact that atomic size and crystal structure of Ca and Sr are similar, a possible ternary solid solubility of the third element exists in the Al–Ca and Al–Sr intermetallic compound system. This demands experimental

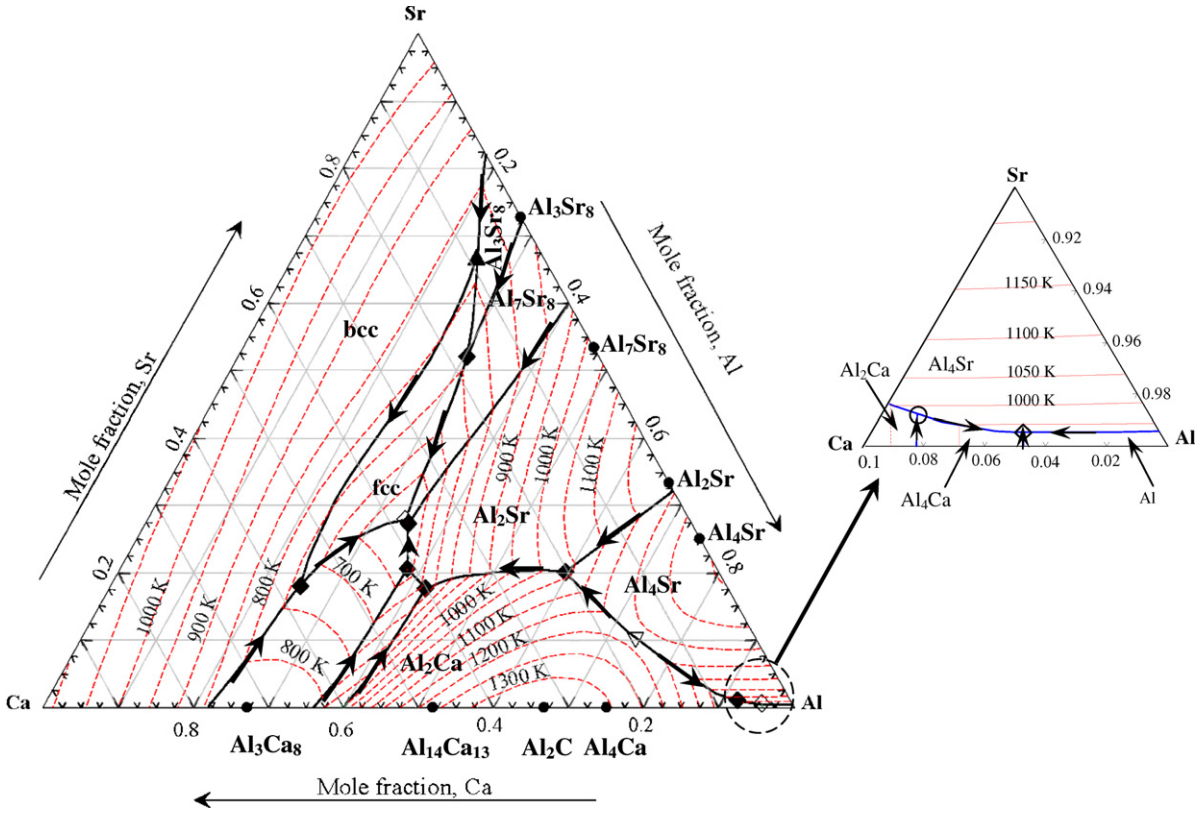

FIGURE 12. Ternary liquidus projection of the Al–Ca–Sr system in mole fraction with invariant points. ○: Ternary quasi-peritetic; ◇, ternary eutectic; ▽: saddle point; ⊗: ternary peritectic.

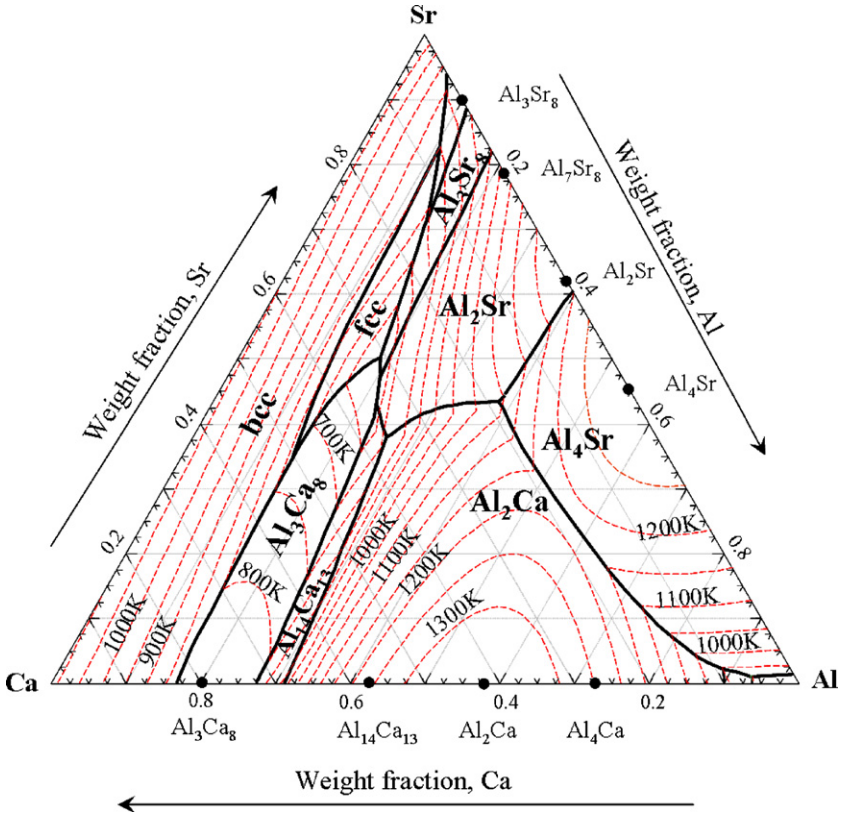

FIGURE 13. Ternary liquidus projection of the Al–Ca–Sr system in weight fraction.

TABLE 4
Ternary invariant points of the Al–Ca–Sr system (atom %)

Reaction	at.% Al	at.% Ca	at.% Sr	T/K	Reaction type[a]
$L \leftrightarrow Al + Al_4Sr + Al_4Ca$	95.39	4.13	0.48	898.55	E1
$L \leftrightarrow fcc + Al_3Ca_8 + Al_7Sr_8$	34.29	37.78	27.93	585.85	E2
$L + Al_3Ca_8 \leftrightarrow fcc + bcc$	25.21	56.72	18.07	726.65	U1
$L + Al_7Sr_8 \leftrightarrow Al_3Ca_8 + Al_2Sr$	35.02	37.72	27.26	587.65	U2
$L + Al_3Ca_8 \leftrightarrow Al_2Sr + Al_{14}Ca_{13}$	38.14	41.24	20.62	620.75	U3
$L + Al_2Sr \leftrightarrow Al_2Ca + Al_{14}Ca_{13}$	42.12	40.23	17.65	710.95	U4
$L + Al_2Ca \leftrightarrow Al_2Sr + Al_4Sr$	59.47	20.46	20.07	1030.85	U5
$L + Al_4Sr \leftrightarrow Al_4Ca + Al_2Ca$	91.89	7.05	1.06	962.45	U6
$L + Al_3Sr_8 \leftrightarrow fcc + Al_7Sr_8$	30.40	17.58	52.02	758.25	U7
$L + bcc + Al_3Sr_8 \leftrightarrow fcc$	24.45	8.94	66.61	810.75	P
$L \leftrightarrow Al_4Sr + Al_2Ca$	73.62	16.02	10.36	962.65	S

[a] E denotes ternary eutectic reaction; U denotes ternary quasi-peritectic reaction; P denotes peritectic reaction; and S denotes saddle point.

investigation in order to determine their solubility limit and the invariant points.

5. Summary

A self-consistent thermodynamic database has been constructed for the Al–Ca–Sr system using the modified quasichemical model. The model parameters are evaluated by incorporating all experimental data available in the literature. The phase diagrams and thermodynamic properties of all the three binaries show good agreement with the experimental data. The ternary phase diagram of the Al–Ca–Sr system is calculated by combining the parameters of the three constituent binaries in one database. The established database for this system predicted one saddle point, one peritectic, seven quasi-peritectics, and two ternary eutectics. This is the first attempt to construct the ternary phase diagram of the Al–Ca–Sr system using the modified quasichemical model and lays the foundation for more developed evaluation.

Acknowledgement

This study is carried out with financial supports from NSERC and NATEQ.

References

[1] E. Baril, P. Labelle, M.O. Pekguleryuz, JOM 55 (2003) 34–39.
[2] M.O. Pekguleryuz, J. Renaud, TMS (2000) 279–284.
[3] D. You, H.S. Schnyders, J.B. Van Zytveld, J. Phys. Condens Mat. 9 (1997) 1407–1415.
[4] A.D. Pelton, P. Chartrand, Metal. Mater. Trans. A 32A (2001) 1355–1360.
[5] A.D. Pelton, S.A. Degterov, G. Eriksson, C. Robelin, Y. Dessureault, Metal. Mater. Trans. B 31B (2000) 651–659.
[6] B.P. Burylev, A.V. Vakhobov, T.D. Dzhuraev, Russ. J. Appl. Chem. 48 (1974) 809–811.
[7] A.V. Vakhobov, T.T. Dzhuraev, B.N. Vigdorovich, Russ. J. Appl. Chem. 48 (1974) 1306–1308.
[8] A.V. Vakhobov, K.K. Eshonov, T.D. Dzhuraev, Russ. Metall. 4 (1979) 167–172 (English Translation).
[9] C. Wolverton, X.Y. Yan, R. Vijayaraghavan, V. Ozolins, Acta Mater. 50 (2002) 2187–2197.
[10] B.Q. Huang, J.D. Corbett, Inorg. Chem. 37 (1998) 5827–5833.
[11] D. Kevorkov, R. Schmid-Fetzer, Z. Metallkd. 92 (2001) 946–952.
[12] G. Bruzzone, F. Merlo, J. Less-Common Met. 39 (1975) 1–6.
[13] B. Closset, H. Dugas, M. Pekguleryuz, J.E. Gruzleski, Metal. Mater. Trans. A 17A (1986) 1250–1253.
[14] E. Sato, N. Kono, I. Sato, H. Watanbe, Chiba Inst. Technol. 35 (1985) 71–78.
[15] M.D. Hanna, A. Merlo, Alloy Phase Diagram, Symp., NY (1983) 411–416.
[16] C.B. Alcock, V.P. Itkin, Bull. Alloy Phase Diagram 10 (1989) 624–630.
[17] P. Chartrand, A.D. Pelton, J. Phase Equilibr. 15 (1994) 591–605.
[18] Y. Zhong, C. Wolverton, Y.A. Chang, Z.K. Liu, Acta Mater. 52 (2004) 2739–2754.
[19] C. Wang, Z. Jin, Y. Du, Alloy. Compd. 358 (2003) 288–293.
[20] F. Sommer, J.J. Lee, B. Predel, Z. Metallkd. 74 (1983) 100–104.
[21] Y.O. Esin, V.V. Litovski, S.E. Demin, M.S. Petrushevski, Russ. J. Appl. Chem. 59 (1985) 446.
[22] A.V. Vakhobov, T.D. Dzhuraev, V.A. Bardin, G.A. Zademidko, Russ. Metall. 1 (1975) 163–166.
[23] S. Srikanth, K.T. Jacob, Z. Metallkd. 82 (1991) 675–683.
[24] L. Donski, Z. Anorg. Allg. Chem. 57 (1908) 201–205.
[25] K. Matsuyama, Sci. Rep. Tohoku Univ. 17 (1928) 783–789.
[26] H. Nowotny, E. Wormnes, E. Mohrnheim, Z. Metallkd. 32 (1940) 39–42.
[27] E.D. Trubnyakova, N.A. Alekseeva, Yu.B. Lyskova, A.V. Vakhobov, I.N. Ganiev, Dokl. Akad. Nauk. Tadzh. SSR 22 (1979) 672–674.
[28] G. Falkenhagen, W. Hofmann, Z. Metallkd. 43 (1952) 69–81.
[29] J.D. Edwards, C.S. Taylor, Trans. Am. Electrochem. Soc. 50 (1926) 391–397.
[30] J.C. Jaquet, H. Warlimont, Z. Metallkd. 72 (1981) 13–20.
[31] M. Notin, J.C. Gachon, J. Hertz, J. Chem. Thermodyn. 14 (1982) 425–434.
[32] M. Notin, J.C. Gachon, J. Hertz, CALPHAD 6 (1982) 49–56.
[33] E. Velesckis, J. Less-Common Met. 80 (1981) 241–255.
[34] P.V. Kocherov, Yu.M. Gertman, P.V. Geld, Zh. Neorg. Khim. 4 (1959) 1106–1112.
[35] S.K. Preto, L.E. Ross, A.E. Martin, M.F. Roche, Proc. Inter. Energ. Conv. Eng. 77 (1977) 241–255.
[36] D. Kevorkov, R. Schmid-Fetzer, A. Pisch, F. Hodaj, C. Colinet, Z. Metallkd. 92 (2001) 953–958.
[37] K.T. Jacob, S. Srikanth, Y. Waseda, J. Jpn. Inst. Met. 29 (1988) 50–59.
[38] E. Schürmann, C.P. Fünders, H. Litterscheidt, Arch. Eisenhuttenews 46 (1975) 473–476.
[39] K. Ozturk, L.Q. Chen, Z.K. Liu, J. Alloy. Compd. 340 (2002) 199–206.
[40] J.G. Schottmiller, A.J. King, F.A. Kanda, J. Phys. Chem. 62 (1958) 1446–1449.
[41] M.W. Chase, Bull. Alloy Phase Diagrams 4 (1983) 123–124.
[42] R.P. Elliott, Constitution of Binary Alloys, First Supplement, McGraw-Hill Book Comp., New York, 1965.
[43] J.F. Smith, O.N. Carlson, R.W. Vest, J. Electrochem. Soc. 103 (1956) 409–413.
[44] D.T. Peterson, V.G. Fattore, J. Phys. Chem. 65 (1961) 2062–2064.
[45] A.J. King, J. Am. Chem. Soc. 64 (1942) 1226–1227.
[46] W. Klemm, G. Mika, Z. Anorg. Allg. Chem. 248 (1941) 155–166.
[47] C.B. Alcock, V.P. Itkin, Bull. Alloy Phase Diagrams 7 (1986) 455–457.
[48] B. Predel, F. Sommer, J. Phys.-Condens. Mat. 17 (1974) 249–265.
[49] A.T. Dinsdale, CALPHAD 15 (1991) 317–425.
[50] M. Blander, J. Braunstein, Ann. N.Y. Acad. Sci. 79 (1960) 838–852.
[51] R.H. Fowler, E.A. Guggenheim, Statistical Thermodynamics, Cambridge University Press, Cambridge, UK, 1939, pp. 350–366.
[52] C.W. Bale, P. Chartrand, S.A. Degterov, G. Eriksson, K. Hack, R. Ben Mahfoud, J. Melançon, A.D. Pelton, S. Petersen, CALPHAD 26 (2002) 189–228.
[53] G.W. Toop, Trans. Am. Inst. Min., Metall. Petr. Eng. 233 (1965) 850–854.

JCT 07-210